Dynamics and Failure of Cylindrical Shells Subjected to Axial Impact

G. Maymon* and A. Libai†
Technion – Israel Institute of Technology, Haifa, Israel

Time history of the expected values of stresses and radial displacements in imperfect, closely spaced, stiffened cylindrical shells subjected to axial impact is analyzed. The analysis is based on Donnell-type equations for the dynamics of stiffened (and unstiffened) cylindrical shells with assumed statistical distributions of the initial imperfections, leading to a statistical description of the response. An engineering-oriented failure criterion is utilized for practical purposes. A specially constructed computer program is utilized for presenting several numerical parametric studies of axially stiffened shells. Of interest is the apparent existence of an optimal size of stiffening.

Nomenclature

$a_{m,n}$ = Fourier coefficients of initial imperfections
D = rigidity of shell, $Eh^3/12(1-\nu^2)$
E = Young's modulus
F = stress function
$C_{m,n}$ = Fourier coefficients for the stress function
$g_{m,n}$ = amplification of the (m,n)th mode
h = shell thickness
$K_{m,n}$ = "rigidity" of (m,n)th mode
L = length of shell
m = number of longitudinal half-waves
n = number of circumferential full waves
N = axial force per unit length, positive in compression
$p_{m,n}$ = frequency of the (m,n)th mode
R = radius of shell
$R_{(\ ),(\ )}$ = expected number of zero crossings
S = ratio between axial stress and classical buckling stress
t = time
t_0 = duration of step loading
w = radial displacement (positive inward)
w_0 = initial radial imperfection
$w_{m,n}$ = Fourier coefficients of radial displacement
x = longitudinal coordinate
y = circumferential coordinate
Z_B = Batdorf parameter $= \sqrt{1-\nu^2}\,(R/h)\,(L/R)^2$
ϕ_n = phase angle
$\lambda_{(\ ),(\ )}$ = expected wavelength
ν = Poisson's ratio
ρ = specific density
σ = stress
σ_{app} = axially applied stress
σ_{cl} = classical buckling stress $= (Eh/R)[3(1-\nu^2)]^{-1/2}$
σ_{VM} = Von Mises stress
σ_x = longitudinal stress
σ_y = circumferential stress
$\sigma(m,n), \sigma_m, \sigma_n$ = standard deviations

Stiffener Nomenclature

In the following, $i=1$ refers to axial stiffeners, whereas $i=2$ refers to circumferential stiffeners (rings):

A_i = area of stiffener
b_i = stiffener spacing
e_i = distance between shell midsurface and the c.g. of the stiffener, positive for internal stiffeners
I_i = moment of inertia of stiffener
$\bar{h}$ = $h[1+(A_1/b_1h)+(A_2/b_2h)]$
η_{0i} = $12(1-\nu^2)[(I_i/b_ih^3)+(A_i/b_ih)(e_i/h)^2]$
η_{ti} = torsional rigidity of stiffener
μ_i = $(1-\nu^2)A_i/b_ih$
χ_i = $(1-\nu^2)(A_i/b_ih)e_i$
ζ_i = $(12/h^2)\chi_i$
β = $[(1+\mu_1)(1+\mu_2)-\nu^2]^{-1}$

I. Introduction

THE design of stiffened and unstiffened cylindrical shells subjected to axial impact poses difficult problems for the design engineer. These relate to the description of the behavior of the shell, the definition of appropriate failure criteria, the influence of the level and duration of the loading on the load-carrying capacity, and the effects of the realistic, imperfect, and not completely known shell geometry on its performance.

Under some widely used assumptions and limitations to be defined later, this paper attempts to cope with some of the problems by presenting a design-oriented analysis of cylindrical shells under axial impact. More specifically, the objectives of this study as are follows:

1) To present a mathematical model for the behavior of cylindrical shells under axial impact, in which statistical characteristics of initial imperfections are included. This model is to be simple enough to permit parametric studies of the effects of shell geometry, stiffener characteristics, and different initial imperfections on the expected values of deformations, stresses, and wavelengths, using an engineering-oriented failure criterion.

2) To present a digital computer program, with which practical application of the model can be made, and to show some results of a parametric study for different shells.

Shells that fail under impact loading exhibit well-defined permanent buckles. For relatively thick shells, plastic buckling dominates, and the initial elastic deformation may

Received Jan. 13, 1977; revision received June 17, 1977.
Index categories: Structural Dynamics; Structural Stability.

*Department of Aeronautical Engineering; presently at the School of Aerospace Engineering, Georgia Institute of Technology, Atlanta, Ga.

†Professor, Department of Aeronautical Engineering. Member AIAA.

be disregarded. For the thin shells that are common in aerospace applications, the final pattern is determined by the early elastic behavior, and hence the elastic dynamic buckling pattern is of prime importance, even if failure occurs eventually through plastic deformations.

Early experimental results[1,2] have shown the familiar diamond pattern of large-deflection static buckling. The diamonds for the dynamic buckling were, however, found to be smaller than in the static case, presumably due to the dominant response of the higher modes to the dynamic loading.

In the past, failure was defined as the occurrence of an accelerated and unbounded growth of deformations.[3] This mathematical criterion is not always applicable to practical cases, since frequently failure of the structure due to excess stresses (or, at least, passage to an inelastic state of stress) may occur in a region where the mathematical solution of the problem is bounded and linear. The present work emphasizes this point, and a more practical and flexible failure criterion is adopted. To some extent, this study is an extension of the basic studies of Lindberg and Herbert.[4,5]

II. Shell Equations

Linearized Donnell-type equations for eccentrically stiffened cylindrical shells with closely spaced stiffeners were derived by Baruch and Singer[6] and subsequently applied to static buckling and vibration problems. In the equations, the closely spaced stiffeners are "smeared" over the shell surface. In order to obtain reasonable results, at least two stiffeners should be contained within a given wavelength. This number becomes highly significant in the region of short wavelengths and presents a limitation to the use of the present theory. The other well-known limitations of the Donnell equations apply as well.

Introducing inertia loads and a stress function F defined by

$$\frac{\partial^2 F}{\partial y^2}=\frac{N_x}{h};\quad \frac{\partial^2 F}{\partial x^2}=\frac{N_y}{h};\quad \frac{\partial^2 F}{\partial x\partial y}=-\frac{N_{xy}}{h} \tag{1}$$

into the Donnell equations with smeared stiffeners,[6] the following equilibrium and compatibility equations, respectively, are obtained:

$$D\nabla^4 w+D\{\eta_{01}w_{,xxxx}+\eta_{02}w_{,yyyy}+(\eta_{t1}+\eta_{t2})w_{,xxyy}-\beta[(1+\mu_2)\zeta_1\chi_1 w_{,xxxx}-2\nu\zeta_1\chi_2 w_{,xxyy}+(1+\mu_1)\zeta_2\chi_2 w_{,yyyy}]\}$$
$$-\beta\{\chi_1[(1+\mu_2)hF_{,yyxx}-\nu hF_{,xxxx}]+\chi_2[(1+\mu_1)hF_{,yyxx}-\nu hF_{,yyyy}]\}-(hF_{,xx}/R)+N[w_{,xx}-w_{0,xx}]+\rho\bar{h}w_{,tt}=0 \tag{2a}$$

$$[(1-\nu^2)/E]\{(1+\mu_2)F_{,yyyy}+(1+\mu_1)F_{,xxxx}+2[(1/\beta(1-\nu))-\nu]F_{,xxyy}\}$$
$$-\nu\chi_1 w_{,xxxx}-\nu\chi_2 w_{,yyyy}+[(1+\mu_2)\chi_1+(1+\mu_1)\chi_2]w_{,xxyy}+(1/\beta R)w_{,xx}=0 \tag{2b}$$

where the prime followed by x or y denotes partial differentiation. Expanding the imperfection data and the solution as Fourier series

$$w_0=\sum_m\sum_n a_{m,n}\sin\frac{m\pi x}{L}\cos\left(\frac{ny}{R}-\phi_n\right),\quad w=\sum_m\sum_n w_{m,n}\sin\frac{m\pi x}{L}\cos\left(\frac{ny}{R}-\phi_n\right),\quad F=\sum\sum C_{m,n}w_{m,n}\sin\frac{m\pi x}{L}\cos\left(\frac{ny}{R}-\phi_n\right) \tag{3}$$

and substituting into the differential equations (1) and (2), the expression for $C_{m,n}$ becomes

$$C_{m,n}=\frac{\dfrac{E}{(1-\nu^2)R\beta}\left(\dfrac{m\pi}{L}\right)^2+\dfrac{Eh}{(1-\nu^2)}\left\{\nu\dfrac{\chi_1}{h}\left(\dfrac{m\pi}{L}\right)^4+\nu\dfrac{\chi_2}{h}\left(\dfrac{n}{R}\right)^4-\left[(1+\mu_2)\dfrac{\chi_1}{h}+(1+\mu_1)\dfrac{\chi_2}{h}\right]\left(\dfrac{\pi mn}{LR}\right)^2\right\}}{(1+\mu_1)\left(\dfrac{m\pi}{L}\right)^4+2\left[\dfrac{1+\nu}{(1-\nu^2)\beta}-\nu\right]\left(\dfrac{\pi mn}{LR}\right)^2+(1+\mu_2)\left(\dfrac{n}{R}\right)^4} \tag{4}$$

Also, the following set of equations is obtained for $w_{m,n}$:

$$\ddot{w}_{m,n}+K_{m,n}w_{m,n}=(N/\rho\bar{h})(m\pi/L)^2 a_{m,n} \tag{5}$$

where $K_{m,n}$ is a "rigidity" given by

$$\frac{\sqrt{3(1-\nu^2)}}{\pi^2}\cdot\frac{R}{h}\frac{\rho L^2}{E}K_{m,n}=\frac{\pi^2}{4\sqrt{3}}\frac{1}{Z_B}\frac{h}{\bar{h}}\left\{\left[m^2+\left(\frac{Ln}{R\pi}\right)^2\right]^2+\eta_{01}m^4+\eta_{02}\left(\frac{Ln}{R\pi}\right)^4+(\eta_{t1}+\eta_{t2})\left(\frac{Lmn}{R\pi}\right)^2\right.$$
$$\left.-\beta\zeta_1\chi_1(1+\mu_2)m^4-\beta\zeta_2\chi_2(1+\mu_1)\left(\frac{Ln}{R\pi}\right)^4+2\nu\beta\zeta_1\chi_2\left(\frac{Lmn}{R\pi}\right)^2\right\}+\left[\sqrt{3}(1-\nu^2)\frac{C_{m,n}}{E\bar{h}}-S\right]m^2$$
$$+\sqrt{3}\pi^2\frac{C_{m,n}}{E\bar{h}}\frac{\beta(1-\nu^2)}{Z_B}\left\{\frac{\chi_1}{h}\left[\nu m^4-(1+\mu_2)\left(\frac{Lmn}{R\pi}\right)^2\right]+\frac{\chi_2}{h}\left[\nu\left(\frac{Ln}{R\pi}\right)^4-(1+\mu_1)\left(\frac{Lmn}{R\pi}\right)^2\right]\right\} \tag{5a}$$

Note that $K_{m,n}$ may become negative for some pairs of m,n and/or for certain values of S.

The solution of Eq. (5) is

$$w_{m,n} = \frac{\pi^2}{\sqrt{3(1-\nu^2)}} \frac{h}{R} \frac{E}{\rho L^2} \frac{1}{K_{m,n}} m^2 Sa_{m,n} \begin{cases} 1-\cosh(pt) \\ 1-\cos(pt) \end{cases} \begin{matrix} K<0 \\ K>0 \end{matrix}$$

where

$$p = |K_{m,n}|^{1/2} \tag{6a}$$

Thus, the solution is unbounded in time for negative values of $K_{m,n}$ and bounded for positive values of $K_{m,n}$. Nevertheless, failure may occur in modes where the solution is bounded if the amplitude is high enough.

Defining the amplification factor as the ratio of the "output" deflection to the input imperfection

$$g_{m,n} = w_{m,n}/a_{m,n} \tag{7}$$

the most amplified mode and the region where it is contained may be located. Table 1 shows results for a typical case.

III. Stresses

The "smeared stiffeners" assumption, which was used for calculating the displacements, is inadequate for stress calculations, where discreteness effects must be taken into account. The stresses may be separated into two parts: 1) membrane stresses designated by σ_{0x} and σ_{0y}; and 2) bending stresses designated by σ_{bx} and σ_{by}.

Expressions for σ_{0x}, σ_{0y}, σ_{bx}, and σ_{by} may be obtained by using the basic relations of the theory of shells and the expressions presented in Ref. 7 for the force resultants of eccentrically stiffened shells. Algebraic manipulations yield the following results:

$$\sigma_{0x} = -\beta \frac{Eh}{1-\nu^2} \left[(1-\nu^2+\mu_2) F_y + (1-\nu^2+\mu_2) \frac{\chi_1}{h} \left(\frac{m\pi}{L}\right)^2 + \nu\mu_1 F_x + \nu\mu_1 \frac{\chi_2}{h} \left(\frac{n}{R}\right)^2 \right] \tag{8a}$$

$$\sigma_{0y} = -\beta \frac{Eh}{1-\nu^2} \left[(1-\nu^2+\mu_2) F_x + (1-\nu^2+\mu_1) \frac{\chi_2}{h} \left(\frac{n}{R}\right)^2 + \varphi\nu_2 F_y + \nu\mu_2 \frac{\chi_1}{h} \left(\frac{m\pi}{L}\right)^2 \right] \tag{8b}$$

where

$$F_x = \left(\frac{m\pi}{L}\right)^2 \frac{1-\nu^2}{Eh} C_{m,n} w_{m,n} \tag{9a}$$

$$F_y = \left(\frac{n}{R}\right)^2 \frac{1-\nu^2}{Eh} C_{m,n} w_{m,n} \tag{9b}$$

Note that Eqs. (8) express the contribution of one term (m,n) to the membrane stresses, and summation over all the modes is to be done in order to obtain total values for the stresses.

Table 1 Results for a typical case

t, μsec	Most amplified $(m_0; n_0)$	$g_{m0,\,n0}$	Region
4	200; 0	1.52	Harmonic
6	199; 0	3.0	Harmonic
8	180; 0	4.8	Harmonic
10	168; 0	7.26	Harmonic
12	160; 0	10.57	Hyperbolic
14	154; 0	15.06	Hyperbolic

Bending stresses are calculated from the following expressions:

$$\sigma_{bx} = \frac{Eh}{2(1-\nu^2)} \left(\frac{\partial^2 w}{\partial x^2} + \nu \frac{\partial^2 w}{\partial y^2} \right) \tag{10a}$$

$$\sigma_{by} = \frac{Eh}{2(1-\nu^2)} \left(\frac{\partial^2 w}{\partial y^2} + \nu \frac{\partial^2 w}{\partial x^2} \right) \tag{10b}$$

The maximum stresses in the axial stiffeners and in the rings may be obtained from

$$\sigma_{xs} = \sigma_{0x} - \nu\sigma_{0y} - 2(Z_{\max}/h)(\sigma_{bx} - \nu\sigma_{by}) \tag{11a}$$

$$\sigma_{yR} = \sigma_{0y} - \nu\sigma_{0x} - 2(Z_{\max}/h)(\sigma_{by} - \nu\sigma_{bx}) \tag{11b}$$

where $Z_{\max}$ is the maximum height of the stiffener, measured from the midsurface of the shell. It is positive for internal stiffeners.

IV. Description of Initial Imperfections

In a previous section, the initial distribution of imperfections was defined by the Fourier series described in Eq. (3). The initial imperfection field for a given shell is measurable. Results of such measurements already have been presented in the literature (e.g., Ref. 8). These measurements were always specific to the shells tested in a particular research program. It seems impractical to test all of the individual shells in the production line during the routine process of design and manufacturing. A statistical approach is called for in such cases, where statistical parameters would define the initial imperfection field. These parameters may vary with different production methods, but once they are determined for a given process, a statistical analysis of the response to various external inputs can be performed.

In the present study, a normal distribution for each $a_{m,n}$ of Eq. (3) was assumed. In Ref. 4, the same assumption was made (for unstiffened shells), but the standard deviation for all couples m,n was the same. It appears to be unjustified to assume the same standard deviation for high and low wave numbers. In the present study, the standard deviation can be any function of m,n, so that even a curve fitting of practical measurements can be taken into account. For the numerical examples, the following function was introduced:

$$f_{(m,n)} = \exp\left[-\frac{1}{2} \frac{(m-m_0)^2}{\sigma_m} \right] \cdot \exp\left[-\frac{1}{2} \frac{(n-n_0)^2}{\sigma_n} \right] \tag{12}$$

This function describes a Gaussian bell with standard deviations σ_m and σ_n in the m and n directions, respectively, centered around a given pair (m_0, n_0). Thus, the standard deviation of each $a_{m,n}$ is given by

$$\sigma(m,n) = \sigma_0(m_0,n_0) \times f(m,n) \tag{13}$$

Expression (13) degenerates to the assumption of Ref. 4 if $\sigma_m = \infty$, $\sigma_n = \infty$ are introduced into Eq. (12).

With the preceding definitions, the mean square value of the deflection w becomes

$$\langle w^2 \rangle = \sigma_0^2(m_0,n_0) \cdot \Sigma\Sigma f(m,n) g_{m,n}^2 \tag{14}$$

Now, given a normally distributed quantity u on the shell, its expected number of zero crossings in the x and y directions may be given by the expressions (see also Ref. 9)

$$R_u^x = \frac{L}{\pi} \left[\frac{\langle (\partial u/\partial x)^2 \rangle}{\langle u^2 \rangle} \right]^{1/2} \tag{15a}$$

$$R_u^y = 2R \left[\frac{\langle (\partial u/\partial y)^2 \rangle}{\langle u^2 \rangle} \right]^{1/2} \tag{15b}$$

The corresponding "wavelengths" of this function in the x and y directions are then

$$\lambda_x = 2L/R_u^x; \qquad \lambda_y = 4\pi R/R_u^y \tag{16}$$

These formulas have been adopted in this paper in order to calculate the number of zero crossings and wavelengths for both displacements and stresses. More explicit formulas for the mean square quantities can be found in Ref. 10.

V. Failure Criteria

In many practical engineering applications, a limiting stress is imposed as the design criterion. In some cases, the elastic limit is chosen as an upper bound for the design. Consequently, an expected stress that is approximately one-third of the elastic limit would be the proper failure criterion, implying that in 99.73% (3σ) of the cases the elastic limit would not be exceeded. An equivalent and more appropriate criterion for two-dimensional states of stress is to use one of the yield-surface criteria. A common example would be the Von Mises effective stress. In still other cases, fatigue considerations may predominate, so that an effective "endurance limit" would control the design.

In all of the cases just mentioned, it was implicitly assumed that the stress-oriented design limitation would be reached before any significant nonlinear effects develop. This is true for many practical stiffened configurations. However, in the case of very thin lightly stiffened shells, nonlinear effects might become important before the design limitation is reached. The complexity of nonlinear analysis of stiffened shells in the presence of statistically defined imperfection fields is so great that its routine use is not practical at the present time. A more useful procedure would be to develop "knock-down" factors by considering simple models or experimental results and applying the stress-oriented criterion on an appropriately reduced stress. A similar procedure has been used in the past in stability analysis.

The analysis presented here also has the capability of using excessive displacements as failure criteria. The limiting displacements may be dictated by the functionality of the design or, in some cases, as a limitation to the analysis when inclusion of nonlinear effects become important. In the latter case, the results can serve as indications for the starting point of a much simplified nonlinear model.

VI. Digital Computer Program

Based on the described model, a digital computer program was written which can perform parametric studies and design analyses of stiffened and unstiffened shells with appropriately chosen failure criteria. The input data to the program include shell and stiffener geometry, material properties, information on the normally distributed imperfection [given by m_0, n_0, σ_m, and σ_n of Eq. (12) and the rms values of initial imperfections), and information on the level and duration of the step loading. Using the theory and equations presented previously, the program calculates (as functions of time) the following quantities: the mean square, number of zero crossings, and wavelengths of the displacements, the mean square, number of zero crossings, expected number of maxima, wavelengths, expected distance between maxima and number of maxima above yield for the axial, circumferential, and "Von Mises" stresses.

The program has been written for a CDC 6500 computer. A typical run takes approximately 100 sec, with a required memory of approximately 60K. Memory must be increased if a case of finite-duration square pulse is to be calculated.

VII. Numerical Study and Examples

A. Introduction

In Refs. 10 and 11, numerous examples for different axially stiffened shells with a variety of stiffener geometries were calculated and presented. Only some of the more typical results are presented here. As a rule, the initial imperfection distribution is characterized by five numbers. It has been given the following designation:

$$\begin{Bmatrix} [a_{m,n}/h]_{\text{rms}} \\ \sigma_m, \quad \sigma_n \\ m_0 \quad n_0 \end{Bmatrix}$$

which appears in the figures. If $\sigma_m = \sigma_n = \infty$, a constant standard deviation is to be taken over the whole m,n plane, and the numbers for m_0, n_0 are meaningless. The calculated stress is the "Von Mises stress," which utilizes the expression

$$\langle \sigma_{VM}^2 \rangle = \langle \sigma_x^2 \rangle + \langle \sigma_y^2 \rangle - \sqrt{\langle \sigma_x^2 \rangle \langle \sigma_y^2 \rangle} \tag{17}$$

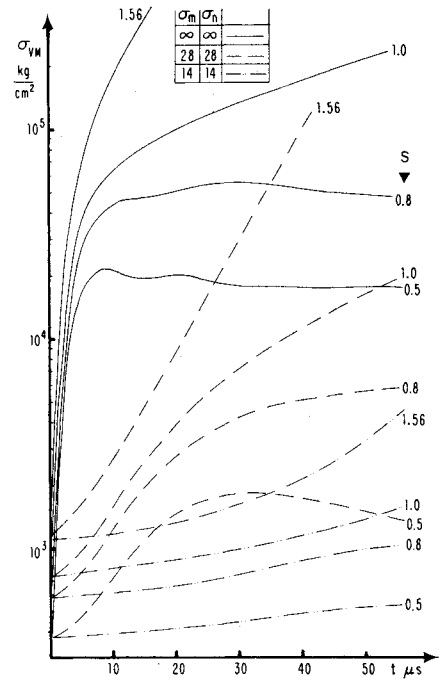

Fig. 1 Effect of load level and initial imperfection distribution on the expected value of stresses in an unstiffened shell.

B. Unstiffened Shells

In Fig. 1, results are presented for the expected values of the "Von Mises stress" for an unstiffened shell with the following geometry: $R = 1.5$ in. $= 3.81$ cm, $L/R = 7.33$, and $R/h = 555$.

Table 2 Initial imperfection data

Case	*A*	*B*	*C*
$(a_{m,n}/h)_{\text{rms}}$	0.1	0.1	0.1
σ_m, σ_n	∞; ∞	28; 28	14; 14
m_0, n_0	Any	2; 2	2; 2

Table 3 Data on stiffeners

	$e_1/h = -1$ (series 1)		$e_1/h = -1.5$ (series 8)		$e_1/h = -2.5$ (series 2)		$e_1/h = -5$ (series 3)	
A_1/bh	Case	I/bh^3	Case	I/bh^3	Case	I/bh^3	Case	I/bh^3
0.2	a_1	0.017	a_2	0.067	a_3	0.267	a_4	1.35
0.6	b_1	0.050	b_2	0.2	b_3	0.800	...	...
1.0	c_1	0.083	c_2	0.333	c_3	1.333	...	...

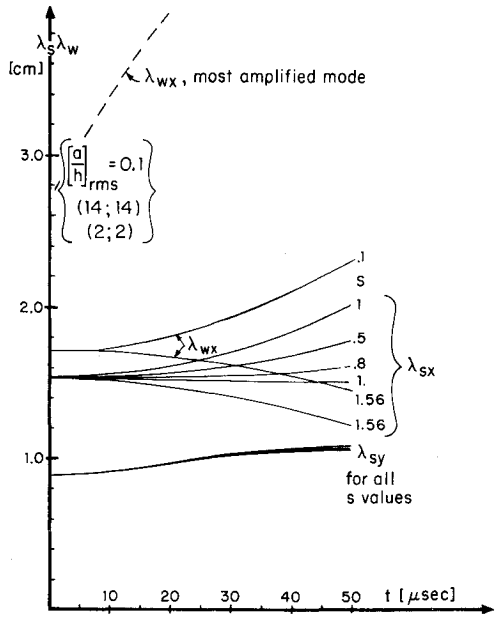

Fig. 2 Expected axial and circumferential wavelengths of "Von Mises stresses" λ_s and of normal displacements λ_w.

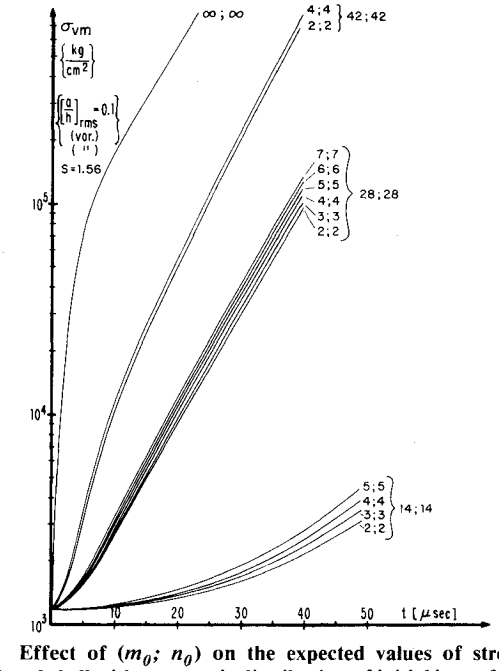

Fig. 3 Effect of $(m_0; n_0)$ on the expected values of stresses for unstiffened shell with symmetric distribution of initial imperfections.

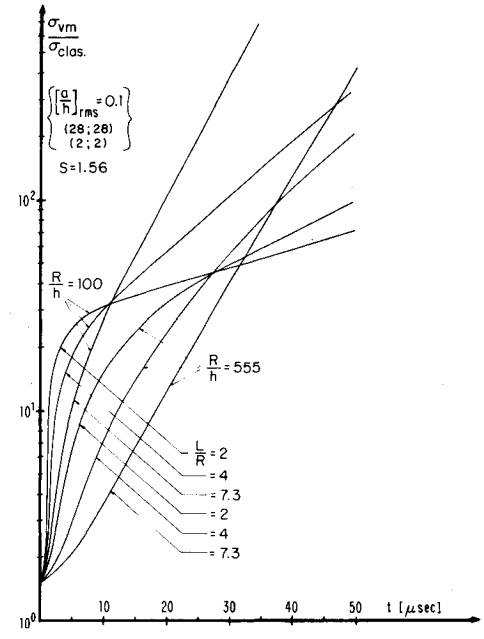

Fig. 4 Effect of nondimensional geometric parameters on expected values of stresses in an unstiffened shell.

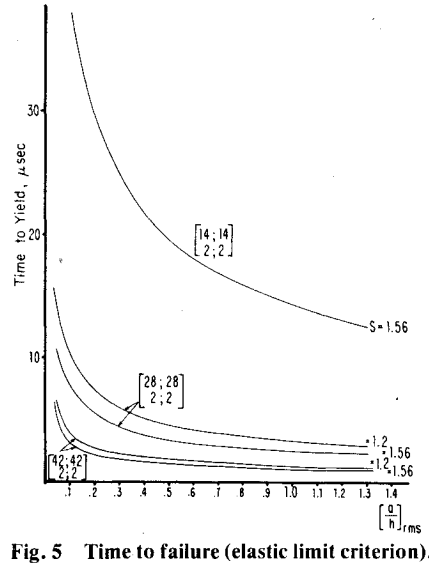

Fig. 5 Time to failure (elastic limit criterion).

The material is aluminum, with the following elastic constants: $E=9.94\times10^6$ psi $=0.7\times10^6$ kg/cm^2, $\nu=0.3$, and with the initial imperfection data given in Table 2.

Calculations were done for several values of axial step loadings, representing fractions of the classical buckling load. In Fig. 2, the expected values for the wavelengths λ_{sx} and λ_{sy} of the "Von Misses stresses" for shell C of Table 2 are presented. Typical results for wavelengths of radial displacement and the wavelength of the most amplified mode (for $s=1.56$) also are presented. In Fig. 3, the effects of different symmetric values of $m_0;n_0$ are shown. The effect of asymmetry in $m_0;n_0$ also was examined but is not presented here. Results can be found in Ref. 11.

In Fig. 4, the effect of changes in the geometrical nondimensional parameters on the expected values of "Von Mises stresses" is shown for a given value of the initial imperfection distribution parameter. For example, defining failure as the exceedance of a "Von Mises stress" value of 6000 kg/cm^2 (85 kpsi), curves similar to those presented in Fig. 5 can be obtained for the time to failure, thus determining the duration of time through which the design is functional.

C. Longitudinally Stiffened Shells

Numerous examples were calculated and presented in Refs. 10 and 11, of which only some typical results are shown here. Only the case of axial stiffening (stringers) was considered. Nominal shell data are as follows:

$$R=6.985 \text{ cm}=2.75 \text{ in.}, \quad R/h=555, \quad L/R=4 \quad Z_B=8480$$

$$(a_{m,n}/h)_{\text{rms}}=0.1, \quad \text{imperfections} \begin{Bmatrix} 28; & 28 \\ 2; & 2 \end{Bmatrix}$$

In Table 3, data for different stiffener geometries are presented. The torsional stiffness of the stiffeners is neglected in all cases ($\eta_{tl}=0$).

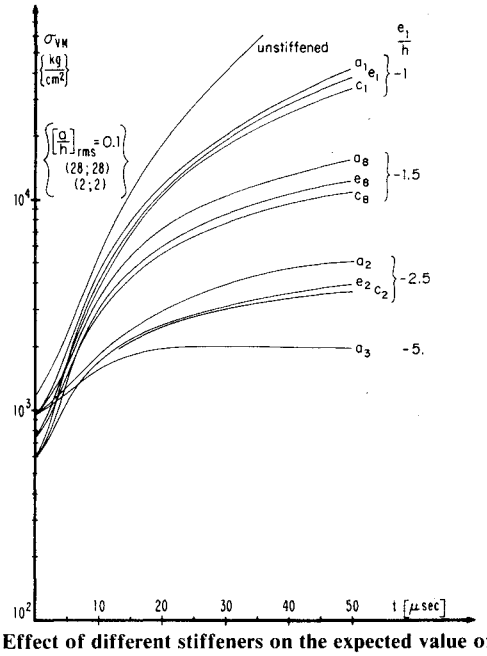

Fig. 6 Effect of different stiffeners on the expected value of stresses in stiffened shells.

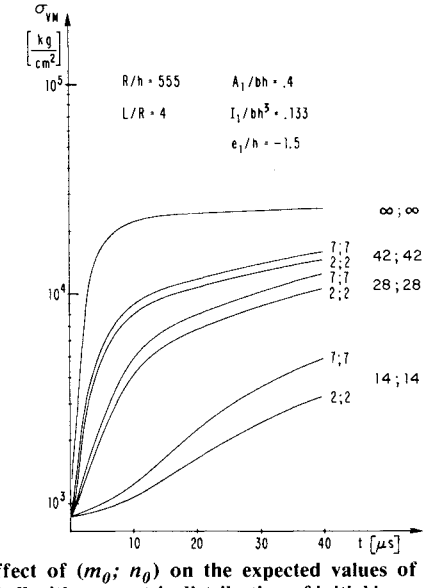

Fig. 7 Effect of (m_0; n_0) on the expected values of stresses in a stiffened shell with symmetric distribution of initial imperfections.

Figure 6 represents results of expected values of stresses in the shell; Fig. 7 shows the effect of m_0; n_0 on these expected stresses for a particular case. It is important to know whether the maximum stresses in the stiffeners are higher or lower than those in the shell itself. Such information may influence the choice of failure allowables and criteria. Calculations were done for several configurations of stiffeners and for several nominal shells, yielding Fig. 8, in which a boundary (with some spread) is shown between regions in which stresses in the shell are higher than those in stiffeners, and vice versa. In most practical cases of closely spaced stiffeners, the design point is in the region of small-eccentricity stiffeners. It should be noted that, since in the higher modes a stiffener with large eccentricity is not fully effective (due to shear lag), the analysis of the higher modes is limited practically to stiffeners with low eccentricity.

In engineering practice, the stiffening of shells is done in order to get more efficient structures. In static cases, the addition of mass usually results in a more rigid geometry and reduces the stresses. In the dynamic case, the addition of mass contributes not only to rigidity forces but also toward additional inertia forces.

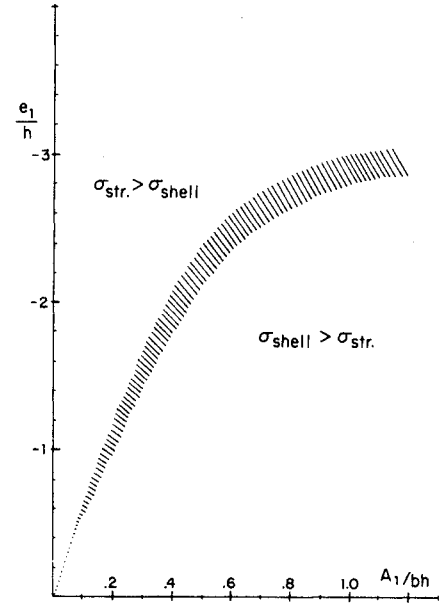

Fig. 8 Relationship between expected values of stresses in the shell and in the stiffener as functions of stiffener parameters.

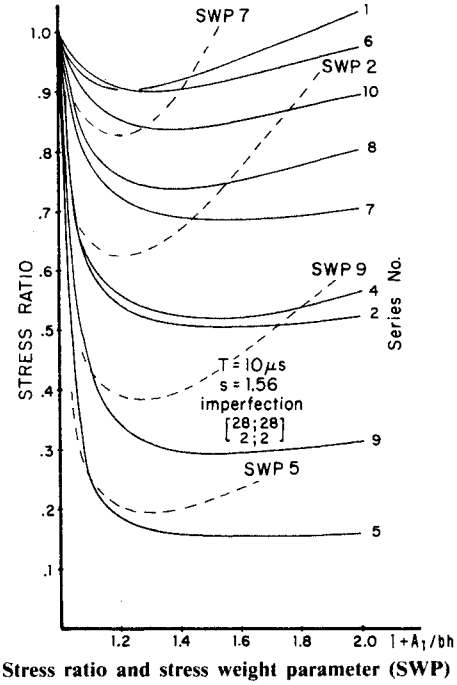

Fig. 9 Stress ratio and stress weight parameter (SWP) for various stiffened shells.

An interesting result is obtained if curves of the stress ratio SR, defined as

$$\text{SR} = \frac{\text{stress in stiffened shell}}{\text{stress in unstiffened shell}}$$

vs the area of the cross section (shells plus stiffeners) are plotted, as was done in Fig. 9 for shells whose geometry is presented in Table 4. A flat minimum is observed in the curves, implying a region of shell geometry where increases in the shell rigidity do not decrease the stresses. This effect is amplified if, for practical purposes of comparison, a weight penalty function is attached to the stress ratio. This "stress weight parameter"

$$\text{SWP} = (\text{SR}) \times (1 + A/bh)$$

may give a more practical description of gains and losses in

Table 4 Different shells and stiffeners data

	R/h	555	100	555
Nominal	L/R	4	2	7.33
shell	Z_B	8480	382	28,500
	-1	Series 1	Series 4	Series 6
e_1/h	-1.5	Series 8	Series 9	Series 10
	-2.5	Series 2	Series 5	Series 7

adding stiffeners to the shell. A plot of this function for several cases is given in Fig. 9.

D. Effects of Load Removal

In Fig. 8, typical results are shown for a step-loading case in which, after $t_0 = 12$ μsec, the load is removed. The solution is based on the homogeneous form of Eq. (5), with the initial conditions for each degree of freedom being obtained from the amplitudes and velocities calculated for the nonhomogeneous solution of Eq. (5) at the time t_0. For comparison, the dashed lines in Fig. 10 describe what would have happened if the load had not been removed.

VIII. Discussion of Numerical Results

It follows from the examples in this paper and Refs. 10 and 11 that the distribution of initial imperfections has a very strong effect on both stress levels and displacements. They both increase with $(\sigma_m;\sigma_n)$. This is due to participation of more modes in the response and can be seen from Figs. 1 and 5. It is interesting to note that even for values of $S<1$, one may still obtain failure due to the engineering-oriented criterion, as discussed in previous sections. It also is noted that, for values of $S<1$, the time history of stresses may have a maximum that is smaller than the yield point. No failure then will occur.

The expected wavelength is not necessarily the one that belongs to the most amplified modes. Also, the change in wavelength with time is very moderate and is influenced little by the value of S. Thus, although time to failure (if any) is affected strongly by S, the failure pattern is not as strongly dependent on the loading level.

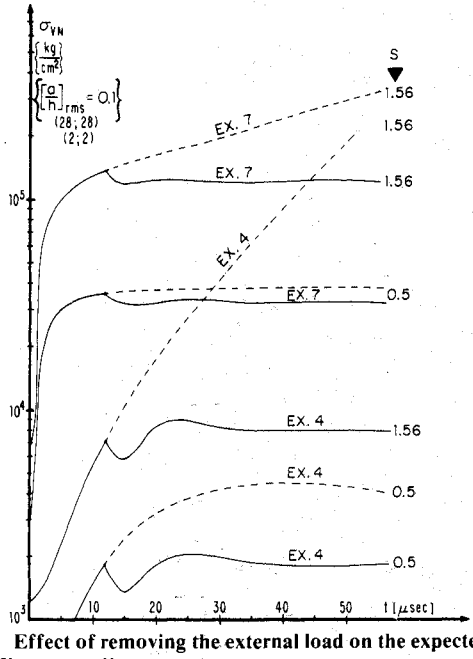

Fig. 10 Effect of removing the external load on the expected value of "Von Mises stress."

There are no large differences between the wavelengths for deformation and wavelengths for stresses, as can be seen by comparing λ_{sx} and λ_{wx} in Fig. 2. From Fig. 3, one may see that, although $(\sigma_m;\sigma_n)$ has a major influence on σ_{VM}, a much smaller effect is contributed by $(m_0;n_0)$ when the pair $(m_0;n_0)$ is small. This seems to be the case in practical shells, whree the most imperfect mode logically is to be found in the small range of $(m_0;n_0)$.

Axial imperfections are more critical for dynamic buckling than the circumferential ones. It can be seen from Ref. 11 that, for small values of σ_m, little dynamic amplification is obtained. The same is true for all values of σ_n (in cases where there are no imperfections in the other direction). The amplification of shorter and thicker shells is higher at the beginning of the process than that of thinner and longer shells (Fig. 4).

Initially, stiffening the shell always reduces the stress levels, but heavier stiffeners do not always imply lower stress levels. In fact, there exists a range of values for A/bh, around 0.2-0.4, which is optimal from the structural dynamics point of view, depending on the optimum criterion to be used.

A practical failure of a structure depends on time. According to the "yield criterion," a structure should not fail during a desired time duration but may fail later, after serving its purpose. Also, a shell that was "condemned" to fail may be saved if the load is removed at the proper time, as may be the case in some practical cases.

Finally, the results stress the importance of the imperfection distribution and of the definition of failure criteria on the dynamic buckling of cylindrical shells. Needless to say, more effort should be invested in the future in establishing methods for the determination of real statistical distributions of imperfections and in experimental verification of the analytical modes of dynamic collapse.

References

[1] Coppa, A.P., "On the Mechanism of Buckling of a Circular Cylindrical Shell under Longitudinal Impact," *10th International Congress of Applied Mechanics,* Stressa, Italy, Aug.-Sept. 1960.

[2] Coppa, A.P., "The Buckling of Circular Cylindrical Shells Subjected to Axial Impact," *Collected Papers on Instability of Shells Structures,* NASA TND-1510, pp. 361-400.

[3] Budiansky, N. and Hutchinson, J.W., "Dynamic Buckling of Imperfection Sensitive Structures," *Proceedings of the 11th International Congress of Applied Mechanics,* Springer Verlag, Berlin, 1967.

[4] Lindberg, H.E., "Dynamic Pulse Buckling of Cylindrical Shells," Poulter Lab., Stanford Research Inst., TR 001-70, 1970.

[5] Lindberg, H. and Herbert, R.E., "Dynamic Buckling of Thin Cylindrical Shells under Axial Impact," *Journal of Applied Mechanics,* Vol. 33, Jan. 1966, pp. 105-112.

[6] Singer, J., Baruch, M., and Harari, O., "On the Stability of Eccentrically Stiffened Cylindrical Shells under Axial Compression," *International Journal of Solids and Structures,* Vol. 3, 1967, pp. 445-450.

[7] Baruch, M. and Singer, J., "Effects of Eccentricity of Stiffeners on the General Instability of Stiffened Cylindrical Shells under Hydrostatic Pressure," *Journal of Mechanical and Engineering Science,* Vol. 5, 1963, p. 23.

[8] Horton, W.H. and Craig, J.I., "Experimental Studies of the Effect of Imperfections on the Elastic Stability of Thin Shells," *Israel Journal of Technology,* Vol. 7, Jan.-Feb. 1969, pp. 91-103.

[9] Rice, S.O., "Mathematical Analysis of Random Noise," *Selected Papers on Noise and Stochastic Processes,* edited by N. Wax, Dover, New York, 1954, pp. 133-294.

[10] Maymon, G., "On the Dynamic Elastic Buckling of Stiffened and Unstiffened Cylindrical Shells under Axial Impact," D.Sc. Thesis, Technion – Israel Inst. of Technology, 1974 (in Hebrew).

[11] Maymon, G. and Libai, A., "On the Dynamic Response and Failure of Stiffened and Unstiffened Cylindrical Shells under Axial Impact," Technion – Israel Inst. of Technology, TAE Rept. 275, March 1976.